

<https://helda.helsinki.fi>

---

## Step-modulated decay cavity ring-down detection for double resonance spectroscopy

Karhu, Juho

2018-10-29

---

Karhu , J , Lehmann , K , Vainio , M , Metsälä , M & Halonen , L 2018 , ' Step-modulated decay cavity ring-down detection for double resonance spectroscopy ' , Optics Express , vol. 26 , no. 22 , pp. 29086-29098 . <https://doi.org/10.1364/OE.26.029086>

---

<http://hdl.handle.net/10138/262550>

<https://doi.org/10.1364/OE.26.029086>

---

cc\_by

publishedVersion

---

*Downloaded from Helda, University of Helsinki institutional repository.*

*This is an electronic reprint of the original article.*

*This reprint may differ from the original in pagination and typographic detail.*

*Please cite the original version.*



# Step-modulated decay cavity ring-down detection for double resonance spectroscopy

JUHO KARHU,<sup>1</sup> KEVIN LEHMANN,<sup>2</sup> MARKKU VAINIO,<sup>1,3</sup> MARKUS METSÄLÄ,<sup>1</sup> AND LAURI HALONEN<sup>1,\*</sup>

<sup>1</sup>*Department of Chemistry, University of Helsinki, Helsinki, Finland*

<sup>2</sup>*Departments of Chemistry and Physics, University of Virginia, Charlottesville, USA*

<sup>3</sup>*Laboratory of Photonics, Tampere University of Technology, Tampere, Finland*

\*[lauri.halonen@helsinki.fi](mailto:lauri.halonen@helsinki.fi)

**Abstract:** A method of measuring double resonant two-photon signal and background from a single cavity ring-down decay is introduced. This is achieved by modulating the double resonance loss via one of the light sources exciting the transition. The noise performance of the method is characterized theoretically and experimentally. The addition of a new parameter to the fitting function introduces a minor noise increase due to parameter correlation. However, the concurrent recording of the background can extend the stable measurement time. Alternatively, the method allows a faster measurement speed, while still recording the background, which is often advantageous in double resonance measurements. Finally, the method is insensitive to changes in the cavity decay rate at short timescales and can lead to improved performance if they have significant contribution to the final noise level compared to the detector noise.

© 2018 Optical Society of America under the terms of the [OSA Open Access Publishing Agreement](#)

## 1. Introduction

Continuous-wave cavity ring-down spectroscopy (CRDS) is a powerful tool for trace gas sensing and measuring weak optical attenuation [1]. In CRDS, light is coupled into a high-finesse optical cavity and the decay of the intracavity power, after the input light is rapidly turned off, is monitored by transmission of one of cavity mirrors. In the case of linear absorption, this light decay is exponential in time and characterized by a decay rate constant which is equal to the fractional optical power loss per round trip times the number of round trips per second (which equals the free spectral range of the cavity). This loss rate, often referred to as the ring-down rate, has a contribution from the finite reflectivity of the mirrors that make up the cavity as well as absorption, scattering, or reflection from any sample inside the cavity. Weak absorption by a gas sample inside the cavity can then be calculated from the difference in the ring-down rate between the cavity with the gas sample and that of the empty cavity. The CRDS method has also been used to measure weak multiphoton transitions, for example in Raman [2] and double resonance spectroscopy [3]. Two-photon transitions can be used to measure spectral features with resolution beyond the Doppler limit [4], without the need of cooling the sample, and they allow accessing energy states that are inaccessible with single photon transitions due to spectroscopic selection rules [5]. Double resonance measurements also provide enhanced selectivity towards the species and eigenstates involved in the transitions, which is of assistance in spectral assignment [6].

The empty cavity ring-down rate typically varies little as a function of the optical frequency compared to gas phase absorption lines. It is often assumed to be a constant and taken to be the ring-down rate when the source frequency is tuned off any molecular resonances, or it is calculated as the constant baseline in a line shape fit. In reality, the empty cavity ring-down rate has been shown to vary in time due to, for example, changes in the measurement environment [7] and it can have some wavelength dependence. Often, output light scattered back into the cavity mode interferes with the field inside the cavity, causing a modulation of the decay rate with the frequency period  $c/2L_{sc}$ , where  $L_{sc}$  is the distance from the cavity output mirror to the scattering source. A change in  $L_{sc}$  of a half wavelength leads to a full period of this modulation in the loss

rate. These drifts in the empty cavity ring-down rate are typically the final limitation in the CRDS sensitivity, particularly when a long averaging time is used. This issue can be alleviated if the total ring-down rate and the empty-cavity ring-down rate can be recorded simultaneously, since their difference can be used to calculate the attenuation coefficient directly. One way to implement this, when recording a spectrum of an absorption line, is to measure the ring-down rate off resonance every other decay and take the difference between the on-resonance and off-resonance decays [7]. This has been shown to improve the optimum averaging time significantly, but it is often considered to be a partial solution, because the two decay times are recorded at slightly different wavelengths and different longitudinal cavity modes. Unless the frequency shift matches the free spectral range of the back scattering contribution to the decay rate, this contribution will not be perfectly canceled. Another method to remove the effects of cavity loss drift is to use saturated absorption cavity ring-down spectroscopy (SCARS) [8]. A saturable absorption will increase in strength during a ring-down decay, leading to a nonexponential decay. By fitting the intensity decay to a model of the saturation, one can separately determine the saturable and nonsaturable contributions to the optical loss. Only near-resonant molecular absorption contributes to the saturable loss. The more complex fitting function in SCARS experiments leads to parameter correlations that increase the uncertainty of the fitting parameter estimators [9], but the trade-off is often advantageous to counter the issues related to the empty-cavity ring-down rate.

Two photon transitions provide another way to distinguish linear from nonlinear cavity losses. For the case of degenerate two photon absorption, where both photons come from a single cavity mode, Lehmann [9] presented an analysis of the predicted cavity decay transient and calculated the expected two photon cross section detection limits as a function of experimental parameters. Another type of two photon spectroscopy is double resonance. Here, one uses a narrow bandwidth laser to selectively pump one particular molecular transition. If this transition is significantly saturated, which requires low pressure, transitions that arise from the same lower state as the pumped transition will be bleached and show a reduction in the absorption coefficient. This is known as V-type double resonance. In addition, new transitions starting from the upper state of the pumped transition, which we call the intermediate state, will appear. If the final state is higher in energy than the intermediate state, the new transition is absorptive; this case is called ladder-type double resonance. If the final state is lower in energy than the intermediate state, the new transition will be stimulated emission, and this is called  $\Lambda$ -type double resonance. Figure 1 shows examples for energy diagrams of the three double resonance types. There are also new absorptions and emissions created by inelastic collisions, which are called four level double resonance. By 100% amplitude modulation of the pump laser, we will ideally selectively modulate only the double resonance transitions, distinguishing them from intrinsic cavity loss, as we well as absorption by other molecules or even other transitions of the molecule being studied.

In this article we consider mostly ladder-type double resonant absorption (DRA) as an example case, but the reasoning is largely general to the other cases of double resonance and other nondegenerate two-photon techniques, such as Raman spectroscopy. In this case, CRDS is used to measure an absorptive transition arising from the pumped intermediate state. The most straightforward way to isolate the double resonance absorption is to measure ring-down decay rate with the pump laser on,  $k_{\text{on}}$ , and with the pump laser off,  $k_{\text{off}}$ , and then the effective double resonance absorption strength,  $\alpha_{\text{dr}}$ , can be calculated

$$\alpha_{\text{dr}} = \frac{n}{c} (k_{\text{on}} - k_{\text{off}}) \quad k_{\text{off}} = (c/n) [(1 - R)/L + \alpha_{\text{linear}}] \quad (1)$$

Here,  $R$  is the reflectivity of the cavity mirrors,  $L$  is their separation,  $n$  is the refractive index,  $c$  is the speed of light, and  $\alpha_{\text{linear}}$  is the linear absorption loss from gases in the cavity. Thus, one needs to make a minimum of two cavity decay measurements to determine  $\alpha_{\text{dr}}$  at any particular optical frequency. Implicit in the use of Eq. 1 is the assumption that the linear losses of the cavity

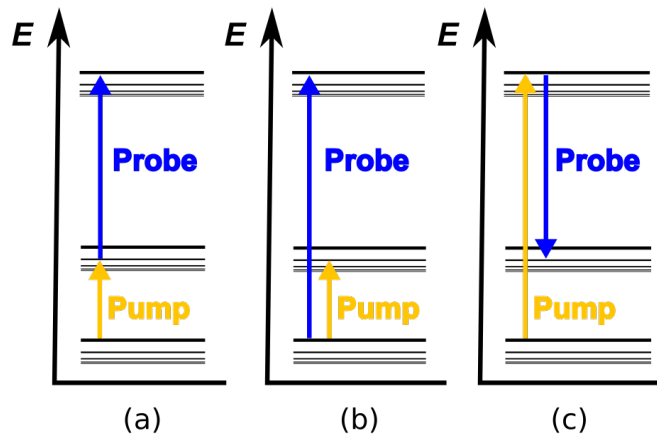


Fig. 1. Energy diagrams for (a) ladder-type double resonant absorption, (b) V-type double resonance, and (c)  $\Lambda$ -type double resonance.

are unchanged in the time interval between measurements and not changed by the presence of the pump laser, which heats the gas if strongly absorbed. For molecules exhibiting slow vibration to rotation and translation (V-RT) relaxation, the pump laser can lead to a substantial build up of population in the lowest vibrationally excited states, as has recently been demonstrated in the case of methane [10]. This disequilibrium occurs on the timescale of V-RT relaxation, which can take tens of thousands of collisions for molecules without low frequency vibrational modes. Some of the “shot to shot” variation of the cavity loss rate can arise from acoustic and vibrational disturbances. These are expected to be uncorrelated for different cavity decay events, which typically occur at the rates of 10-1000 times per second.

A potential way to reduce the above effects on the precision that  $\alpha_{\text{dr}}$  can be determined is to modulate the pump laser intensity during each cavity decay. Figure 2 shows the principle of this measurement scheme. For clarity and brevity, we will refer to this method as Step-Modulated decay cavity Ring-down Spectroscopy (SMRS). With this method, the decay rates  $k_{\text{off}}$  and  $k_{\text{on}}$  will be determined with a time separation on the order of the cavity decay time, which is typically in the 10-100  $\mu\text{s}$  range. Since this can be much shorter than the thermal relaxation times, and even the V-RT rates of the gas, the method could lead to an increase in sensitivity. A theoretical analysis was done on the predicted standard error in the difference of  $k_{\text{on}}$  and  $k_{\text{off}}$ , and will be presented below. In the ideal case (with no drift in the cavity loss), it is found that the SMRS approach gives somewhat higher standard errors than subtracting the loss rates from two complete decays, but the increase is modest.

Even without an increase in sensitivity, the SMRS has an advantage in that one needs to observe only a single decay at each wavelength. Double resonance experiments are Doppler free as the pump laser will pump only molecules with the correct velocity component in the propagation direction of the pump beam, to within the power broadened homogeneous width of the pump transition. When the molecular collisional mean free path is significantly less than the transverse width of the pump laser, the degree of optical saturation scales inversely with the square of the pressure. As a result, such experiments are usually carried out at low sample pressure where the homogeneous width is less than 1% of the Doppler broadened width. This narrow width, up to a factor of the ratio of the probe frequency divided by the pump frequency, is transferred to the double resonance transitions, which are typically only a few MHz wide [11]. This is an asset to double resonance experiments, allowing increased spectroscopic resolution

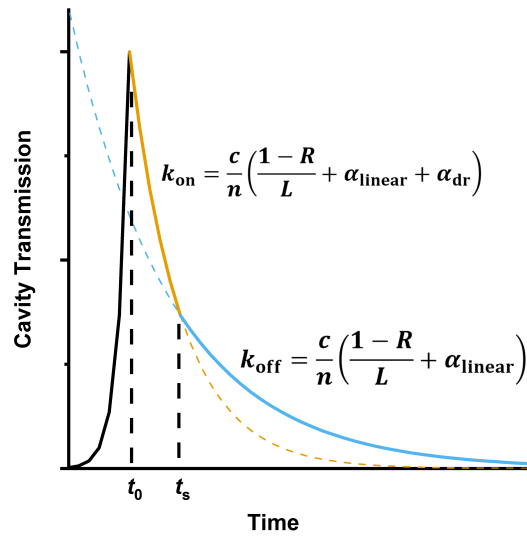


Fig. 2. Principle of the SMRS. In the beginning of the ring-down decay, one light source, referred to as the pump, is exciting one step of the double resonance, and the second step is excited by the light source of the CRDS measurement. During the initial phase of the decay, the ring-down time is affected by the cavity loss, linear absorption of the sample gas and possible double-resonant two-photon loss. In the middle of the decay, the pump laser is turned off. After this point, the ring-down time is determined by the cavity loss and the linear absorption only. The two ring-down times can be used to calculate the double resonance loss.

and allowing for unambiguous discrimination of collision induced four level double resonance transitions, which are Doppler broadened. However, it does mean that one must take frequency steps of the probe laser that are on the order of 1 MHz or less, and observe ring-down events at each step. If the signal to noise ratio is sufficient, SMRS allows one to scan a spectrum at twice the rate compared to the case where separate pump and no-pump cavity decays are measured. The fast scan speed can be especially advantageous when measuring narrow sub-Doppler transitions, since instabilities in the pump laser wavelength and power may degrade the line shape during the scan over the transition line profile. This degradation can be alleviated for example by using stabilized lasers to excite the transitions, but this generally requires significantly more complex measurement setups [3].

Below, we will introduce the theoretical model used for fitting the SMRS decay. We will also derive theoretical results for how the noise of SMRS compares to that of normal CRDS. Afterwards, we present experimental results in the form of an example DRA spectrum measured with SMRS, as well as experimental results showing how using SMRS may affect the measurement noise.

## 2. Fitting model and theoretical analysis

We assume that we digitize the signal produced by the photo-detector/amplifier monitoring the cavity intensity decay with a rate of  $\Delta t^{-1}$ , where  $\Delta t$  is the time step between two measured points. The recorded ring-down traces are fitted with the nonlinear least squares method. For  $t \leq t_s = N_1 \Delta t$ , we assume the cavity intensity decays with the rate  $k_{on}$ . At the time  $t_s$ , the pump laser is turned off and for  $t > t_s$ , the decay rate is  $k_{off}$ . Assume that we digitize  $N_2$  points after

the switch. To keep the model simple we have assumed that the turn on/off of the pump laser as well as the time for the system to relax to the new steady state is small relative to  $\Delta t$  so that we do not have to model the transition between pumped and nonpumped states. If we define the time of transition as  $\Delta t_t$ , our approximation should be accurate as  $k_{\text{on}}\Delta t_t \ll 1$  and  $k_{\text{off}}\Delta t_t \ll 1$ . We define running integer variables  $0 \leq i < N_1$  and  $0 \leq j < N_2$ , with  $t_i = i\Delta t$  and  $t_j = (N_1 + j)\Delta t$ . The  $N_1 + N_2 + 1$  digitized detector voltage values are fitted to the functional form  $S_{i,j}$  with:

$$S_i = A \exp(-k_{\text{on}}\Delta t i) + B \quad 0 \leq i < N_1 \quad (2)$$

$$S_j = A \exp(-k_{\text{on}}\Delta t N_1 - k_{\text{off}}\Delta t j) + B \quad 0 \leq j < N_2 \quad (3)$$

In each cycle of the nonlinear least square fit to the data, corrections to the optimized parameters are given by  $\Delta \vec{p} = \alpha^{-1} \cdot \vec{\beta}$ . The curvature matrix  $\alpha$  is a symmetric  $N_p \times N_p$  matrix where  $N_p$  is the number of fitting parameters. Its elements are given by  $\alpha_{p1,p2} = \sum_i \frac{\partial S_i}{\partial p1} \frac{\partial S_i}{\partial p2} + \sum_j \frac{\partial S_j}{\partial p1} \frac{\partial S_j}{\partial p2}$ , where  $p1$  and  $p2$  are fitting parameters. The sums over  $i$  and  $j$  can be considered finite power series of variables  $\exp(-k_{\text{on}}\Delta t)$  and  $\exp(-k_{\text{off}}\Delta t)$ , and their closed form solutions can be evaluated using expressions for geometric series and its derivatives. Elements of the vector  $\vec{\beta}$  are given by  $\beta_p = \sum_i (y_i - S_i) \left( \frac{\partial S_i}{\partial p} \right) + \sum_j (y_j - S_j) \left( \frac{\partial S_j}{\partial p} \right)$ . The vector  $y$  contains the measured point of the ring-down decay. The expressions for the closed form solutions of  $\alpha$  and  $\vec{\beta}$  are presented in Appendix I.

Under the assumptions that the data points have uncorrelated, Gaussian random noise with variance  $\sigma_d^2$ , and it is small enough that the linearization around the least square fit parameter values is accurate for noise deviations of the data, we can calculate the predicted variance of the fitting constants from the covariance matrix,  $\epsilon = \sigma_d^2 \alpha^{-1}$ . The diagonal elements of  $\epsilon$  are the variances of the respective parameters and the off-diagonal elements give the covariances. In particular, the variance of  $\Delta k = k_{\text{on}} - k_{\text{off}}$  is predicted to be  $\epsilon_{k_{\text{on}},k_{\text{on}}} + \epsilon_{k_{\text{off}},k_{\text{off}}} - 2\epsilon_{k_{\text{on}},k_{\text{off}}}$ .

In the limit of optimal measurement conditions, where the ring-down decay is recorded long enough ( $k\Delta t N_2 \gg 1$ ) and with small enough time step relative to the decay constant ( $k\Delta t \ll 1$ ), the expression for the variance of  $\Delta k$  is given by:

$$\sigma^2(\Delta k) = \frac{4k^3 \Delta t}{e^{-2kt_s} - e^{-4kt_s} (2k^2 t_s^2 + 2kt_s + 1)} \left( \frac{\sigma_d}{A} \right)^2 \quad (4)$$

We assume here that the two decay rate constants are the same  $k = k_{\text{on}} = k_{\text{off}}$ . The expression has a minimum at  $kt_s = 0.8966$ , which gives us the optimal switching time as just short of one decay time constant. The variance at the minimum is  $\sigma^2(\Delta k) = 89.83 \times k^3 \Delta t \left( \frac{\sigma_d}{A} \right)^2$ . Previously it was shown that with normal CRDS at the same limit, the variance of the decay rate constant is  $\sigma^2(k) = 8k^3 \Delta t \left( \frac{\sigma_d}{A} \right)^2$  [12]. Therefore, the standard deviation of the double resonance signal from SMRS is predicted to be about 3.35 times larger than absorption coefficient measured with traditional CRDS. It should be noted that, if  $k_{\text{on}}$  and  $k_{\text{off}}$  are measured with separate single exponential fits, two decays need to be measured. Taking their difference introduces a noise increase of a factor of  $\sqrt{2}$  due to uncorrelated noise. Additionally, two modulated SMRS decays could be measured in the same period of time, decreasing the measurement noise, also by the factor of  $\sqrt{2}$ . Altogether, the SMRS is predicted to have a noise increase of about a factor of 1.675, relative to measuring  $k_{\text{on}}$  and  $k_{\text{off}}$  from separate single exponential CRDS decays. Figure 3 shows the standard deviation of  $\sigma^2(\Delta k)$ , relative to the single exponential case, as a function of the switching time. It can be seen that the standard deviation is insensitive to the exact switching time, as long as its near the optimal value.



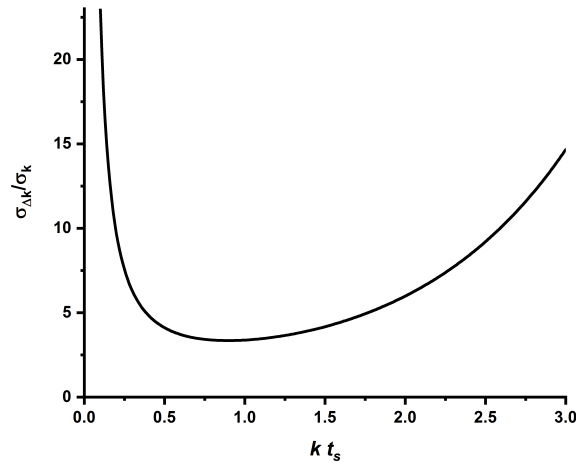


Fig. 3. Standard deviation of the difference between  $k_{\text{on}}$  and  $k_{\text{off}}$ , compared to the standard deviation of decay rate  $k$  from a single exponential decay, as a function of the switching time. Switching time  $t_s$  is the point at which the modulated decay changes from rate  $k_{\text{on}}$  to  $k_{\text{off}}$ . The time axis has been normalized to the decay rate.

### 3. Experimental setup and double resonance measurement

Figure 4 shows a schematic picture of the measurement setup. One light source is a continuous-wave mid-infrared optical parametric oscillator (OPO) [13], which is now acting as the pump source in the scheme described above. The probe laser is a near-infrared external cavity diode laser (ECDL; Velocity 6328, New Focus), which is used for the CRDS measurement. The ECDL beam passes through an acousto-optic modulator (AOM). The first order refraction from the AOM is coupled into a fiber to transport the beam to the measurement system. To counteract the losses from fiber coupling, fiber propagation, AOM refraction efficiency and other optics, the fiber output is amplified with an erbium doped fiber amplifier, after which, the beam is passed through mode-matching optics and coupled into the CRDS cavity. The cavity decay is recorded with an amplified photodetector (D100, Redwave labs). The signal is then sent to a comparator circuit, which controls the AOM, and to a computer for data recording and processing. The cavity is brought into resonance with the ECDL wavelength by tuning the cavity length over one free spectral range via a piezo actuator attached to one of the cavity mirrors. When the near-infrared power transmitted through the cavity starts to rise and reaches a specified level, the AOM controlling the ECDL is turned off to initiate the ring-down decay. The OPO beam is also sent through an AOM. The refracted beam is superimposed with the ECDL beam before the CRDS cavity. The CRDS mirrors have high reflectivity (around 0.99998) only in the near-infrared region, but transmit most of the mid-infrared OPO power through the cavity in a single pass.

For the example case, we perform DRA measurement of a vibrational transition of acetylene ( $\text{C}_2\text{H}_2$ ). After initiating the ring-down decay by turning off the AOM controlling the ECDL output, the power transmitted by the cavity back mirror starts to decay. Because the decay during this initial part has contribution from cavity mirror reflectivity, linear absorption, and the possible double resonance loss, the decay rate is the total ring-down rate  $k_{\text{on}}$ . At time  $t_s$ , the AOM controlling the OPO output is also turned off. After this point, the decay is affected only by the empty cavity losses and linear absorption, so the decay rate is the background ring-down rate  $k_{\text{off}}$ . Since it was shown that the optimal value for  $t_s$  is at about one time constant of the decay,

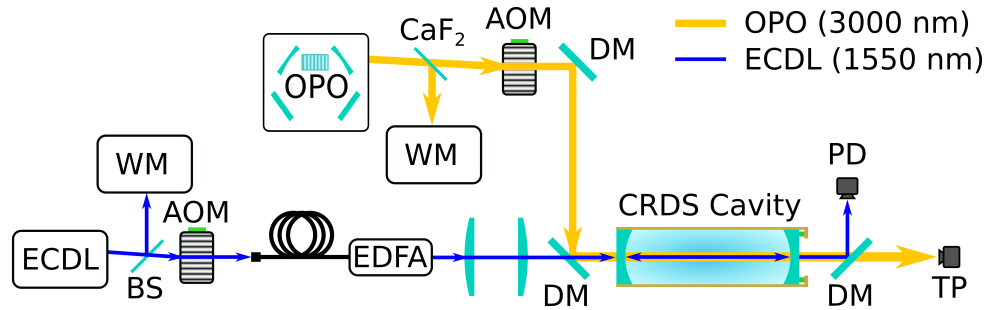


Fig. 4. Schematic of the measurement setup. BS: beam sampler, WM: wavemeter, DM: dichroic mirror, PD: photodiode, TP: thermopile detector.

the AOM controlling the OPO output is triggered when the transmitted power drops to about  $e^{-1} = 0.368$  times the initial amplitude.

Figure 5 shows a DRA spectrum measured with SMRS. The OPO wavelength was tuned to the side of the R(9) line of the  $\nu_3$  fundamental transition of  $C_2H_2$ . The ECDL wavelength was then scanned over the R(10) line of the transition  $\nu_1 + 2\nu_3 \leftarrow \nu_3$ , where  $\nu_1$  is the symmetric and  $\nu_3$  the antisymmetric CH-stretching vibrations in the normal mode notation. The trace labeled  $k_{on}$  in Fig. 5 shows the ring-down time of the initial part of each recorded ring-down decay. This is the part of the ring-down decay, where OPO is exciting the first transition and it shows sharp DRA lines. The spectrum shows typical features of a double resonance transition [5]. At the exact double resonance condition, where the Doppler shifted transition frequency matches both the OPO frequency and the ECDL frequency, there is one sharp Lorentzian feature. The spectrum shows two of these sharp features, symmetrically around the line center. This is because the ECDL forms a standing wave inside the CRDS cavity, so that there are two waves propagating in opposite directions inside the cavity, corresponding to two oppositely signed Doppler-shifts. Because a relatively large scan steps size was used to keep the scanning speed high, the line shapes cannot be resolved in high detail. It can be seen however, that the widths of the two DR lines are different. This is because the linewidth of a DR line depends on the relative directions of the two light sources used for the excitation [11]. There is also a weak Doppler broadened feature between the two peaks, which is often seen in double resonance spectra. This is likely caused by partial thermalization of the population of the intermediate state, for example due to collisions or radiation trapping. The trace labeled  $k_{off}$  is the ring-down rate for the part of the decay after the OPO was turned off. The end of the decay is affected by the empty cavity loss, as well as linear absorption of the gas sample and the shape of this trace shows that the measured DRA transition coincides with the side of a linear absorption line. Nevertheless, the DRA attenuation coefficient can be easily resolved, since the linear absorption affects both traces equally and can be subtracted out. Both ring-down times at each point are taken from a single decay, with no averaging over multiple cavity excitations.

#### 4. Results and discussion

We compared the noise behavior of the decay rate extracted from measured CRDS decay traces using either the classic single exponential fits, or the SMRS fits. We recorded ring-down decays for about 5 hours at a repetition rate of about 3 Hz. The slow repetition rate was chosen to keep the amount of data manageable. Each trace was fitted with both the modulated decay model of SMRS, as well as single exponential decay model for comparison. The cavity was pumped empty and the pump beam was not on in these measurements, so the results reflect how the different



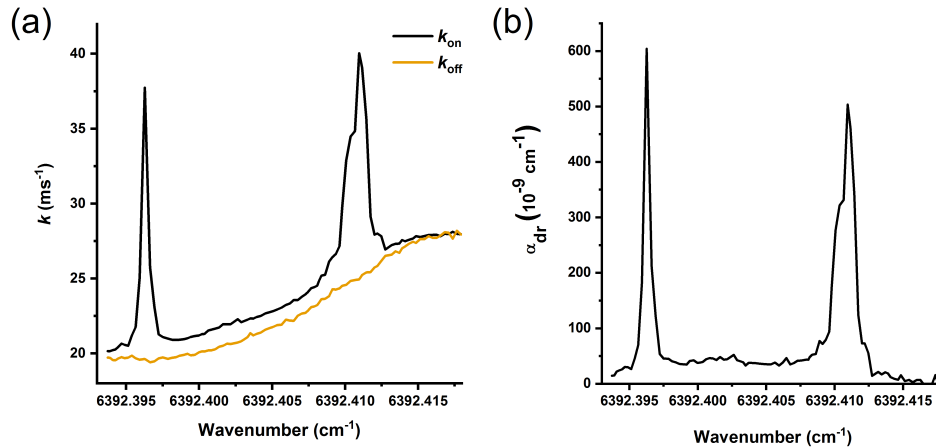


Fig. 5. a) An example ring-down spectrum recorded with the SMRS without averaging. The OPO was on at the beginning of the ring-down decay, corresponding to the  $k_{\text{on}}$  trace. The end of the decay is affected only by the empty cavity losses, as well as any linear absorption of the ECDL that coincides with the double resonance line ( $k_{\text{off}}$  trace). As shown by the shape of the latter trace, here the double resonance line resides at the side of a linear absorption line. b) The double resonance attenuation coefficient calculated from the spectrum on the left.

fits affect the measurement noise in practice. For the SMRS, the two ring-down rates extracted from a single decay should be the same and therefore the noise of their difference reflects on the uncertainty of the modulated fits. For the normal single exponential CRDS, the ring-down rate gives the empty cavity losses and, in the ideal case, it should be a constant over the whole measurement. The results are shown as Allan-Werle deviations in Fig. 6. For the SMRS, the trace is the Allan-Werle deviation of the double resonance absorption coefficient calculated using Eq. 1. For normal CRDS, the Allan-Werle deviation is calculated for the value  $k/c$ , so that units are the same for both traces.

At short averaging times, normal CRDS has lower noise level, by about a factor of 2. This is slightly lower than the factor of 3.35 predicted above. This likely reflects the fact that the noise is not just from the uncertainty of the fit parameter estimators, but the actual ring-down rate has some variation from decay to decay, towards which the SMRS is less sensitive. Possible cause of this is that there is some small wavelength dependency for the mirror reflectivity or some residual absorption, since the laser wavelength is not completely stable. Mechanical and acoustic disturbances may also cause noise in the empty cavity loss at relatively short time scales. On long time scales, the drift of the empty cavity ring-down time becomes clear as the Allan-Werle deviation of CRDS starts to increase, while the noise of SMSR keeps decreasing. This behavior shows the typical advantage of simultaneously measuring both the total ring-down rate and the background ring-down rate, namely the better stability at the long time scale, allowing for example, a longer optimal averaging time. In double resonance measurements, this advantage is likely situational, since one often wants to pass over the resonance fast with only short averaging times. If one has access to particularly stable light sources or if the spectral features to be measured are much broader than the linewidth of the light sources, as may be the case in, for example, stimulated Raman transitions [2], the longer averaging time could provide an advantage in terms of the ultimate sensitivity that can be reached.

As noted above, the SMRS is expected to be less susceptible to short term noise and variation

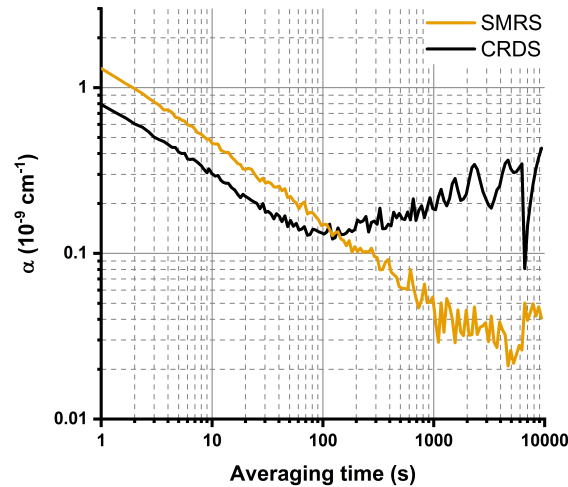


Fig. 6. Allan-Werle deviation of attenuation coefficient measured with traditional CRDS and SMRS. The CRDS-trace is the deviation for the variable  $k/c$ , where  $k$  is the ring-down rate, measured with normal CRDS. The SMRS-trace is the deviation for double resonance absorption coefficients from modulated decay fits. The data for both models were the same set of ring-down decays, recorded over about 5 hours. The ECDL was kept free running at around a set wavelength during the whole measurement and OPO was off the whole time.

of the ring-down rate from decay to decay. As a demonstration of this, we measured again the noise behavior at a single ECDL wavelength without the pump beam, but we deliberately increased the decay to decay variation of the ring-down rate. A low pressure acetylene sample was introduced to the cavity and the ECDL wavelength was tuned to a side of a linear absorption line. The laser frequency tuning was fed with noise from an arbitrary waveform generator. The ECDL linewidth is typically about 1-2 MHz on the time scale between the cavity excitations. The linewidths were estimated by measuring the beat note between the laser and a stabilized frequency comb (FC1500-250-WG, Menlo Systems). When the laser frequency tuning was fed with white noise with root mean square power of 50 mV, the ECDL linewidth increased to about 10 MHz. Due to the slope of the absorption line, this corresponded to a spread in the ring-down rates of about  $0.15 \text{ ms}^{-1}$ . The average ring-down rate at the ECDL wavelength used in the measurements was about  $22 \text{ ms}^{-1}$ .

The data were again fitted using both the single exponential CRDS model and the SMRS model. The noise performance with and without the added wavelength noise is shown in Fig. 7 as Allan-Werle deviations. This time, the CRDS trace shows the difference between two ring-down rates, measured from consecutive decays, to simulate the measurement of DRA loss. The idea is that the one decay trace gives the total ring-down rate and another is used to measure the background ring-down rate. This method should show similar long term performance as SMRS, although the measurement time is prolonged. Here we are interested in the noise at the short time scale. Note, however, that since the OPO is again off in the measurements, the ring-down rate of the two decays should be the same and the results only reflect on the noise performance of the method. Note also that here the averaging time takes into account the fact that it takes twice as long to measure one point with normal CRDS, since two decays need to be measured to get  $\alpha_{\text{dr}}$ . This leads to a decrease in the relative noise of SMRS compared to the normal CRDS approach as was already mentioned above.

It can be seen that without the added wavelength noise, SMRS performs slightly worse at

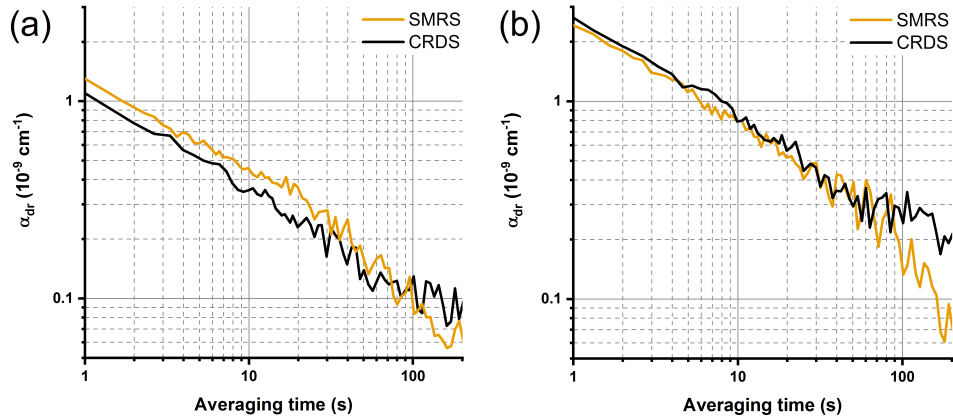


Fig. 7. Allan-Werle deviations for double resonance absorption measured either using two separate single exponential decays (CRDS-trace) or SMRS method, to measure the total losses and only the linear losses. The ECDL was again kept at constant wavelength and OPO was not used. The ECDL wavelength was chosen so that it coincided with a side of an absorption line. a) the ECDL is free-running, with its typical narrow linewidth. b) excess noise has been added to the ECDL wavelength, resulting in about 10 MHz linewidth. The wavelength noise couples into variation of the ring-down rate between decays.

low averaging times, as was expected. However, when the increased linewidth leads to a larger variation of the ring-down rate from decay to decay, the order of the traces change. There is an increase in the noise for both traces, so SMRS is not completely immune to these kinds of noisy conditions, but it is less sensitive to them.

## 5. Conclusion

We have shown that simultaneous recording of the background using SMRS leads to longer stability of the measurement system. Additionally, and uniquely to two-photon transitions, the spectral interference from nearby absorption lines can be alleviated, when the linear absorption can be included in the background ring-down rate. The performances are similar when comparing SMRS to measuring the total and background ring-down time from separate decays. The latter method has typically slightly lower measurement noise, but SMRS is less susceptible to actual variation of the empty cavity ring-down time. Additionally, SMRS can be used for faster measurements, which is often advantageous in double resonance spectroscopy. In general, if the performance with short averaging times is limited by the detection noise, the advantage of using SMRS is likely limited to the increased scanning speed. If the actual variation of the ring-down rate is a major contributor to the noise of the measurement, SMRS can lead to improved noise performance as well.

## Appendix I

For the linearized least squares fits, we require the elements of the Jacobian matrices  $J_{i,k}$  and  $J_{j,k}$  which are the partial derivatives of the model functions  $S_i$  and  $S_j$  with respect to the  $k$ 'th model parameter. We will assume that each data point has the same Gaussian random noise with root mean squared value of  $\sigma$ . In this case, all the data points are equally weighted. To simplify the notation, we introduce auxiliary variables  $a_1 = \exp(-k_1 \Delta t)$  and  $a_2 = \exp(-k_2 \Delta t)$ , where  $k_1$  is the decay rate for the initial part of the decay and  $k_2$  is the decay rate for the latter part. We have

Jacobian matrix elements given by:

$$\begin{aligned}
 \frac{\partial S_i}{\partial B} &= 1 & \frac{\partial S_j}{\partial B} &= 1 \\
 \frac{\partial S_i}{\partial A} &= a_1^i & \frac{\partial S_j}{\partial A} &= a_1^{N_1} a_2^j \\
 \frac{\partial S_i}{\partial k_1} &= -A \cdot \Delta t \cdot i \cdot a_1^i & \frac{\partial S_j}{\partial k_1} &= -A \cdot \Delta t \cdot N_1 \cdot a_1^{N_1} \cdot a_2^j \\
 \frac{\partial S_i}{\partial k_2} &= 0 & \frac{\partial S_j}{\partial k_2} &= -A \cdot \Delta t \cdot j \cdot a_1^{N_1} \cdot a_2^j
 \end{aligned} \tag{5}$$

The curvature matrix is a symmetric  $N_p \times N_p$  matrix where  $N_p$  is the number of fitting parameters, with elements given by  $\alpha_{p1,p2} = \sum_i \frac{\partial S_i}{\partial p1} \frac{\partial S_i}{\partial p2} + \sum_j \frac{\partial S_j}{\partial p1} \frac{\partial S_j}{\partial p2}$ . The sums over  $i$  and  $j$  can be evaluated in closed form using the properties of a geometric series and its derivatives.. These are given by

$$\begin{aligned}
 \alpha_{B,B} &= N_1 + N_2 \\
 \alpha_{A,B} &= \frac{1 - a_1^{N_1}}{1 - a_1} + a_1^{N_1} \frac{1 - a_2^{N_2}}{1 - a_2} \\
 \alpha_{k_1,B} &= -A \cdot \Delta t \left[ \frac{a_1 \cdot (1 - a_1^{N_1}) - N_1 a_1^{N_1} (1 - a_1)}{(1 - a_1)^2} + N_1 a_1^{N_1} \cdot \frac{1 - a_2^{N_2}}{1 - a_2} \right] \\
 \alpha_{k_2,B} &= -A \cdot \Delta t \cdot a_1^{N_1} \cdot \left[ \frac{a_2 \cdot (1 - a_2^{N_2}) - N_2 \cdot a_2^{N_2} \cdot (1 - a_2)}{(1 - a_2)^2} \right] \\
 \alpha_{A,A} &= \frac{1 - a_1^{2N_1}}{1 - a_1^2} + a_1^{2N_1} \frac{1 - a_2^{2N_2}}{1 - a_2^2} \\
 \alpha_{k_1,A} &= -A \cdot \Delta t \cdot \left[ \frac{a_1^2 \cdot (1 - a_1^{2N_1}) - N_1 a_1^{2N_1} (1 - a_1^2)}{(1 - a_1^2)^2} + N_1 a_1^{2N_1} \frac{1 - a_2^{2N_2}}{1 - a_2^2} \right] \\
 \alpha_{k_2,A} &= -A \cdot \Delta t \cdot a_1^{2N_1} \cdot \left[ \frac{a_2^2 \cdot (1 - a_2^{2N_2}) - N_2 \cdot a_2^{2N_2} (1 - a_2^2)}{(1 - a_2^2)^2} \right] \\
 \alpha_{k_1,k_1} &= (A\Delta t)^2 \left[ \frac{a_1^2 (1 + a_1^2) - a_1^{2N_1} \left[ N_1^2 (1 - a_1^2)^2 + 2N_1 a_1^2 (1 - a_1^2) + a_1^2 (1 + a_1^2) \right]}{(1 - a_1^2)^3} \right. \\
 &\quad \left. + N_1^2 a_1^{2N_1} \frac{1 - a_2^{2N_2}}{1 - a_2^2} \right] \\
 \alpha_{k_1,k_2} &= (A\Delta t)^2 N_1 a_1^{2N_1} \left[ \frac{a_2^2 (1 - a_2^{2N_2}) - N_2 a_2^{2N_2} (1 - a_2^2)}{(1 - a_2^2)^2} \right] \\
 \alpha_{k_2,k_2} &= (A\Delta t)^2 a_1^{2N_1} \left[ \frac{a_2^2 (1 + a_2^2) - a_2^{2N_2} \left[ N_2^2 (1 - a_2^2)^2 + 2N_2 a_2^2 (1 - a_2^2) + a_2^2 (1 + a_2^2) \right]}{(1 - a_2^2)^3} \right]
 \end{aligned} \tag{6}$$

We also need the  $N_p$  element vector with elements  $\beta_p = \sum_i (y_i - S_i) \left( \frac{\partial S_i}{\partial p} \right) + \sum_j (y_j - S_j) \left( \frac{\partial S_j}{\partial p} \right)$ . These elements can be expressed as:

$$\begin{aligned}
 \beta_B &= \sum_i y_i + \sum_j y_j - A \left[ \frac{1 - a_1^{N_1}}{1 - a_1} + a_1^{N_1} \frac{1 - a_2^{N_2}}{1 - a_2} \right] - B [N_1 + N_2] \\
 \beta_A &= \sum_i y_i a_1^i + \sum_j y_j a_2^j - A \left[ \frac{1 - a_1^{2N_1}}{1 - a_1^2} + a_1^{2N_1} \frac{1 - a_2^{2N_2}}{1 - a_2^2} \right] - B \left[ \frac{1 - a_1^{N_1}}{1 - a_1} + a_1^{N_1} \frac{1 - a_2^{N_2}}{1 - a_2} \right] \\
 \beta_{k_1} &= -A\Delta t \left[ \sum_i y_i \cdot i \cdot a_1^i + N_1 a_1^{N_1} \sum_j y_j a_2^j \right] \\
 &\quad + A^2 \Delta t \left[ \frac{a_1^2 (1 - a_1^{2N_1}) - N_1 a_1^{2N_1} (1 - a_1^2)}{(1 - a_1^2)^2} + N_1 a_1^{2N_1} \frac{1 - a_2^{2N_2}}{1 - a_2^2} \right] \\
 &\quad + B \cdot A \cdot \Delta t \left[ \frac{a_1 (1 - a_1^{N_1}) - N_1 a_1^{N_1} (1 - a_1)}{(1 - a_1)^2} + N_1 a_1^{N_1} \frac{1 - a_2^{N_2}}{1 - a_2} \right] \\
 \beta_{k_2} &= -A\Delta t a_1^{N_1} \sum_j y_j \cdot j \cdot a_2^j + A^2 \Delta t a_1^{2N_1} \left[ \frac{a_2^2 (1 - a_2^{2N_2}) - N_2 a_2^{2N_2} (1 - a_2^2)}{(1 - a_2^2)^2} \right] \\
 &\quad + AB\Delta t a_1^{N_1} \left[ \frac{a_2 (1 - a_2^{N_2}) - N_2 a_2^{N_2} (1 - a_2)}{(1 - a_2)^2} \right] \tag{7}
 \end{aligned}$$

In each cycle of the nonlinear least square fit to the data, corrections to the fitting parameters are given by  $\Delta \vec{p} = \alpha^{-1} \cdot \vec{\beta}$ .

If we include a variable baseline value,  $B$ , the fit, we have four fitting parameters. If we fix the baseline at a specific value, then we remove the  $B$  row and column of the  $\alpha$  matrix and the  $B$  element of  $\beta$ . Measurement of the deep tail of the decay, or better yet, the data when the input laser is blocked, provides a way to determine  $B$  and  $\sigma$ , thereby breaking the fitting correlation of  $B$  with the decay rates.

## Funding

CHEMS doctoral program of the University of Helsinki; the Finnish Cultural Foundation; the Academy of Finland (294752).

## References

1. D. Romanini, A. A. Kachanov, N. Sadeghi, and F. Stoeckel, "CW cavity ring down spectroscopy," *Chem. Phys. Lett.* **264**, 316–322 (1997).
2. F. V. Englich, Y. He, and B. J. Orr, "Continuous-wave cavity-ringdown detection of stimulated Raman gain spectra," *Appl. Phys. B* **94**, 1–27 (2008).
3. J. Karhu, M. Vainio, M. Metsälä, and L. Halonen, "Frequency comb assisted two-photon vibrational spectroscopy," *Opt. Express* **25**, 4688–4699 (2017).
4. W. K. Bischel, P. J. Kelly, and C. K. Rhodes, "Observation of Doppler-free two-photon absorption in the  $\nu_3$  bands of  $\text{CH}_3\text{F}$ ," *Phys. Rev. Lett.* **34**, 300–303 (1975).
5. M. Siltanen, M. Metsälä, M. Vainio, and L. Halonen, "Experimental observation and analysis of the  $3\nu_1(\Sigma_g)$  stretching vibrational state of acetylene using continuous-wave infrared stimulated emission," *J. Chem. Phys.* **139**, 054201 (2013).

6. A. Callegari, H. K. Srivastava, U. Merker, K. K. Lehmann, G. Scoles, and M. J. Davis, "Eigenstate resolved infrared-infrared double-resonance study of intramolecular vibrational relaxation in benzene: First overtone of the CH stretch," *J. Chem. Phys.* **106**, 432–435 (1997).
7. H. Huang and K. K. Lehmann, "Long-term stability in continuous wave cavity ringdown spectroscopy experiments," *Appl. Opt.* **49**, 1378–1387 (2010).
8. G. Giusfredi, S. Bartalini, S. Borri, P. Cancio, I. Galli, D. Mazzotti, and P. De Natale, "Saturated-absorption cavity ring-down spectroscopy," *Phys. Rev. Lett.* **104**, 110801 (2010).
9. K. K. Lehmann, "Theoretical detection limit of saturated absorption cavity ring-down spectroscopy (SCAR) and two-photon absorption cavity ring-down spectroscopy," *Appl. Phys. B* **116**, 147–155 (2013).
10. T. Hausmaninger, G. Zhao, W. G. Ma, and O. Axner, "Depletion of the vibrational ground state of CH<sub>4</sub> in absorption spectroscopy at 3.4 μm in N<sub>2</sub> and air in the 1–100 Torr range," *J. Quant. Spectros. Radiat. Transfer* **205**, 59–70 (2018).
11. J. E. Bjorkholm and P. F. Liao, "Line shape and strength of two-photon absorption in an atomic vapor with a resonant or nearly resonant intermediate state," *Phys. Rev. A* **14**, 751–760 (1976).
12. K. K. Lehmann and H. Huang, "Optimal signal processing in cavity ring-down spectroscopy," in *Frontiers of Molecular Spectroscopy* (Elsevier, 2009), pp. 623–658.
13. M. Siltanen, M. Vainio, and L. Halonen, "Pump-tunable continuous-wave singly resonant optical parametric oscillator from 2.5 to 4.4 μm," *Opt. Express* **18**, 14087–14092 (2010).